Spectroscopic Detection of Transient Thiamin Diphosphate-Bound Intermediates on Benzoylformate Decarboxylase†

Eduard A. Sergienko,‡ Jue Wang,‡ Lena Polovnikova,§ Miriam S. Hasson,*,§ Michael J. McLeish,|| George L. Kenyon,|| and Frank Jordan*,‡

Department of Chemistry and Program in Cellular and Molecular Biodynamics, Rutgers, the State University, Newark, New Jersey 07102, Department of Biological Sciences, Purdue University, West Lafayette, Indiana 47907-1392 and College of Pharmacy, University of Michigan, Ann Arbor, Michigan 48109-1065

Received May 30, 2000; Revised Manuscript Received August 16, 2000

ABSTRACT: Thiamin diphosphate (ThDP)-dependent enzymes catalyze a range of transformations, such as decarboxylation and ligation. We report a novel spectroscopic assay for detection of some of the ThDP-bound intermediates produced on benzoylformate decarboxylase. Benzoylformate decarboxylase was mixed with its alternate substrate *p*-nitrobenzoylformic acid on a rapid-scan stopped-flow instrument, resulting in formation of three absorbing species (λ_{max} in parentheses): I_1 (a transient at 620 nm), I_2 (a transient at 400 nm), and I_3 (a stable absorbance with $\lambda_{max} > 730$ nm). Analysis of the kinetics of the two transient species supports a model in which a noncovalent complex of the substrate and the enzyme is converted to the first covalent intermediate I_1; the absorbance corresponding to I_1 is probably a charge-transfer band arising from the interaction of the thiamin diphosphate-*p*-nitrobenzoylformic acid covalent adduct (2-*p*-nitromandelylThDP) and the enzyme. The rate of disappearance of I_1 parallels the rate of formation of I_2. Chemical models suggest the λ_{max} of I_2 (near 400 nm) to be appropriate to the enamine, a key intermediate in ThDP-dependent reactions resulting from the decarboxylation of the thiamin diphosphate-*p*-nitrobenzoylformic acid covalent adduct. Therefore, the rate of disappearance of I_1 and/or the appearance of I_2 directly measure the rate of decarboxylation. A relaxation kinetic treatment of the pre-steady-state kinetic data also revealed a hitherto unreported facet of the mechanism, alternating active-sites reactivity. Parallel studies of the His70Ala BFD active-site variant indicate that it cannot form the complex reported by the charge-transfer band (I_1) at the level of the wild-type protein.

Direct spectroscopic demonstration of the existence of enzyme-bound intermediates is a particularly powerful and often difficult method of study. The ability to study the time course of their reactions is particularly important for enzymes that utilize coenzymes. In many cases, the coenzyme itself can carry out the overall reaction in the absence of the protein. This is the case of the family of enzymes dependent on thiamin diphosphate (ThDP, the vitamin B1 coenzyme). In the three closely related structures in this family that have been solved, benzoylformate decarboxylase (BFD,[1] see Scheme 1), pyruvate decarboxylase (PDC), and pyruvate oxidase, it is clear that the key residues binding the diphosphate and the aminopyrimidine ring, and enforcing the unusual "V" conformation are conserved, while several other catalytic residues are not conserved. This is consistent with the hypothesis attributing the bulk of the catalytic rate acceleration to the cofactors, as active-site residues change quite drastically between related proteins with only 20−25% sequence identities.

Such direct spectroscopic experiments are particularly important if, as in this family, one is to understand fully the contribution of the protein to the catalytic rate acceleration. The presence of a conjugated intermediate, the C2α-carbanion/enamine, on ThDP-dependent pathways allows the opportunity to carry out such experiments, for neither of the other covalent ThDP-bound intermediates [the ThDP-substrate adduct (C2α-mandelylThDP or MThDP), and the ThDP-product adduct (C2α-hydroxybenzylThDP or HBThDP)] has such conjugation. In earlier studies at Rutgers, advantage was taken of the fact that yeast PDC (*1*−*3*) accepts substrates in which the methyl group of pyruvate is replaced by a ring-substituted styrene group, thereby enabling direct

†This work was supported at Rutgers by Grant USPHS-NIH-GM-50380, the Rutgers Busch Biomedical Fund, the Rutgers Board of Governors Fund, Roche Diagnostics Inc., Indianapolis, IN, and NSF BIR94/13198; at Purdue by NSF Grants 9733552 and 9600876 (to M.S.H.); and at Michigan by Grant USPHS-NIH-GM-40570 (to G.L.K.).

* To whom correspondence should be addressed. For M.S.H., telephone: 765-496-2928; fax: 765-496-1189; e-mail: mhasson@bragg.bio.purdue.edu. For F.J., telephone: 973-353-5470; fax: 973-353-1264; e-mail: frjordan@newark.rutgers.edu.

‡ Rutgers, The State University.

§ Purdue University.

|| University of Michigan.

[1] Abbreviations: BFD, benzoylformate decarboxylase; PDC, yeast pyruvate decarboxylase; NBFA, *p*-nitrobenzoylformic acid; ThDP, thiamin diphosphate; E·NBFA, the Michaelis complex formed between BFD and NBFA; MThDP, C2α-mandelylthiamin diphosphate, the covalent complex formed between benzoylformic acid and ThDP; NMThDP, *p*-nitromandelylThDP; HBThDP, C2α-hydroxybenzylthiamin diphosphate, the covalent complex formed between the benzaldehyde product and ThDP; NHBThDP, the *p*-nitro analogue of HBThDP; BSA, bovine serum albumin; PMSF, phenylmethanesulfonyl fluoride; SDS−PAGE, sodium dodecyl sulfate−polyacrylamide gel electrophoresis.

10.1021/bi001214w CCC: $19.00
Published on Web 10/21/2000

Scheme 1

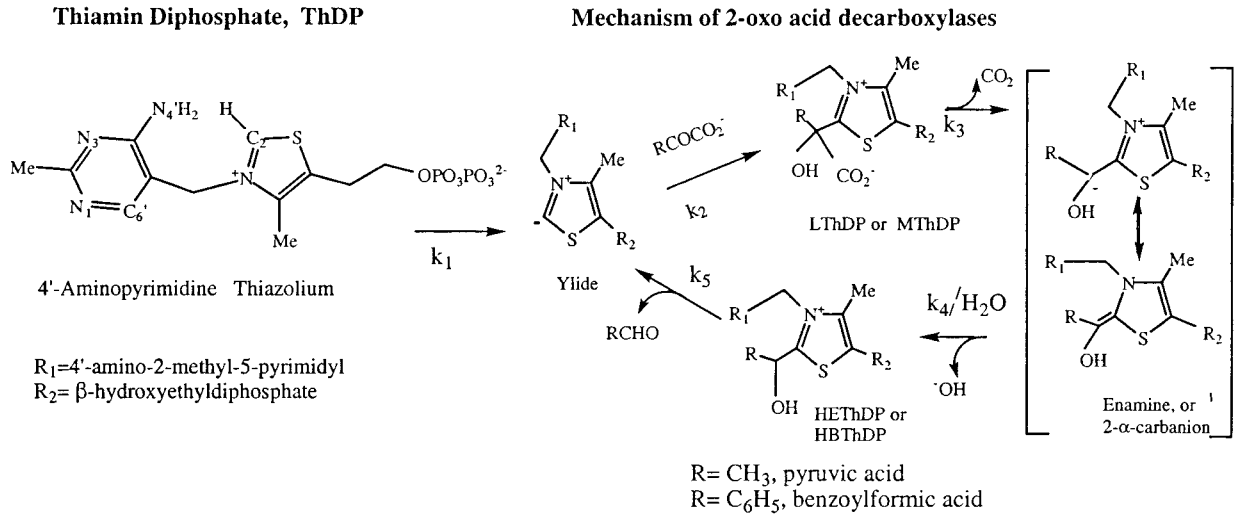

detection of the derived enamine intermediate (*4*−*7*). However, these conjugated analogues of pyruvic acid are very much poorer substrates than pyruvate itself and, while the formation of the enamine from these substrates was shown to proceed at a rate consistent with the enzyme's turnover number (*6*), the eventual kinetic fate of the enamine was difficult to ascertain. The enamine derived from pyruvic acid has a λ_{max} near 290 nm (*8*), overlapping the large protein band, making observation difficult. Benzoylformate, on the other hand, should be decarboxylated by BFD (*9*−*12*) to an enamine with a $\lambda_{max} \geq 380$ nm, depending on the phenyl substituent (*13*, *14*), enabling observation of the enamine from an alternate substrate more structurally similar to the true substrate than previously used on PDC (*4*−*7*). Given the likely presence of such enamine intermediates on all ThDP-requiring enzymes, observation of the kinetic behavior of this intermediate would be of relevance to all such enzymes, but especially to the very large family of 2-oxo acid decarboxylases carrying out both oxidative and non-oxidative chemistry on their substrates.

Here we report observation of the kinetic fate of the enamine derived from *p*-nitrobenzoylformic acid (NBFA) on BFD by rapid-scan stopped-flow spectrophotometry. The chromophoric nature of the substrate analogue gives evidence for two transients and a chromophoric product in the visible spectrum, and their kinetic analysis enabled us to deduce specific rate constants for a number of steps in the pathway. Analysis of a variant BFD, H70A, suggests the steps at which His70 at the active center (see Figure 1) participates in the pathway.

EXPERIMENTAL PROCEDURES

Reagents. Sepharose Q and phenyl Sepharose chromatography resins, molecular weight standard kit for SDS−PAGE, and SDS−PAGE staining dye were purchased from Amersham-Pharmacia. ThDP, kanamycin, benzoylformic acid, and triethanolamine were purchased from Sigma. BSA, PMSF, ampicillin, SDS, acrylamide/bis-acrylamide solution were purchased from Midwest Scientific. Tryptone and yeast extract were obtained from Difco. Sodium phosphate, sodium and potassium hydroxide, hydrochloric and acetic acid, sodium chloride, and ammonium sulfate were obtained from Mallinckrodt. Water was purified with a Nanopure system (Barnstead). All other chemicals used were the highest available purity.

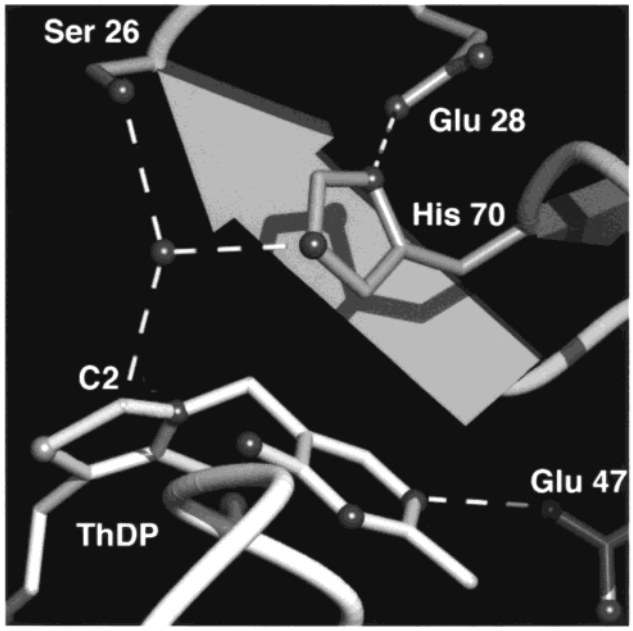

FIGURE 1: Key active center side chains on benzoylformate decarboxylase.

BFD Expression and Purification. The purification protocol for BFD was based on the procedure described previously by Hasson et al. (*17*). All the purification steps were performed at either 4 °C or on ice. An FPLC system (Pharmacia) was used for all chromatography steps. BFD was expressed in *Escherichia coli* M15[pRep7] (Qiagen) containing the plasmid pBFDtrc (*18*). The cells were grown at 37 °C on a shaker in Luria broth in the presence of 100 mg/L ampicillin, 40 mg/L kanamycin, and 2 mg/L thiamin. The cells were induced with 1 mM IPTG at an OD_{600} of 1 and grown for 10−14 h post induction. Typically, 6−9 L of cell culture was used for a single purification. The cells were harvested by centrifugation, frozen in liquid nitrogen, and stored at −80 °C. The frozen cells were thawed, resuspended in 50 mM potassium phosphate, pH 6.0, 0.1 mM ThDP, and

0.1 mM PMSF, and lysed by passing the suspension through the French pressure cell. The lysate was centrifuged at 100000*g* for 90 min, and the supernatant fraction was subjected to 40−80% ammonium sulfate fractionation. The pellet was suspended in 20 mM triethanolamine chloride, pH 7.5, 0.1 mM ThDP (buffer A), and dialyzed against the same buffer. The dialysate was loaded onto a SepharoseQ FPLC column previously equilibrated with buffer A. Following loading, the column was washed with 5 column volumes of buffer A containing 100 mM NaCl, and the protein was eluted with a gradient (40 column bed volumes) of 100−500 mM NaCl in buffer A. BFD eluted between 200 and 250 mM NaCl, as determined by assaying the fractions for BFD enzymatic activity. The BFD-containing fractions were pooled, exchanged by dialysis into 50 mM sodium phosphate, pH 6.0 (buffer B), containing 1 M ammonium sulfate. After loading onto a phenyl Sepharose FPLC column equilibrated with the same buffer, the column was washed with 5 column volumes of the buffer B containing 1 M ammonium sulfate. Prior to elution, ThDP was added to fraction collection tubes so that the final concentration of ThDP in each fraction was 0.2 mM. The protein was eluted with a 1−0 M gradient of ammonium sulfate in buffer B, with BFD eluting between 550 and 250 mM ammonium sulfate, as judged from the absorbance profile of the eluant at 280 nm. The fractions containing BFD were pooled, exchanged by dialysis into 25 mM HEPES, pH 7.0, 0.2 mM ThDP, 0.1 mM $MgCl_2$ and concentrated either by using an Amicon ultrafiltration cell or Amicon Centriprep (TM) concentrators to a final protein concentration of 15−50 mg/mL. The pure enzyme was frozen in aliquots in liquid nitrogen and stored at −80 °C.

Analysis of Enzyme Purity and Activity. Protein concentration was determined by Bradford assay (*16*) using BSA as a standard. In the early stages of protein purification, enzyme activity was determined by direct continuous assay (*10*). Final enzyme activities and steady-state kinetic constants were determined by the horse liver alcohol dehydrogenase/NADH coupled assay (*12*). Protein was analyzed for homogeneity by SDS−PAGE using the mini-gel system purchased from Pharmacia.

Preparation and Purification of the H70A BFD Variant. BFD H70A was prepared using *Pfu* DNA polymerase and the QuikChange site-directed mutagenesis kit (Stratagene, La Jolla, CA). The mutants were constructed using pBFDtrc (*18*) as the DNA template. The forward primer used for the mutagenesis is shown below with the mutated codon underlined, and the lowercase letters indicating a base change from wild type: 5′-GCCGGCTTTCATTAACCTGgcTTCT-GCTGCTGG-3′. In addition to creating the His−Ala mutation, this change in sequence resulted in the loss of a *Bsm*1 restriction site. Following mutagenesis, the template DNA was removed by treatment with *Dpn*1, and the remaining PCR products were transformed into *E. coli* strain XL1-Blue (Stratagene, La Jolla, CA). Single colonies were picked, and their DNA was isolated and screened for the desired mutation by restriction analysis using *Bsm*1. The fidelity of the PCR amplification and the presence of the mutation were confirmed by sequencing. A plasmid containing the mutated BFD was selected and denoted pKKBFDH70A.

This plasmid was used to transform *E. coli* M15 [pRep7], and a single colony was chosen for expression of BFD H70A. The expression and purification were carried out using the same procedure as for the wild-type enzyme (above).

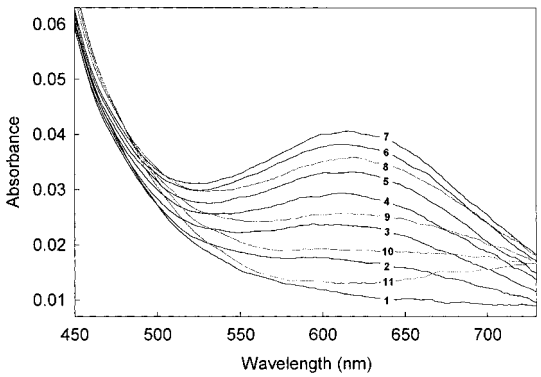

FIGURE 2: Rapid-scan stopped-flow spectrum of wild-type BFD reacting with *p*-nitrobenzoylformic acid at pH 7.0 and 5.6 °C. Concentration of BFD was 5.8 μM and of NBFA was 5 mM. Reaction was carried out in 0.1 M HEPES buffer, containing 1 mM $MgCl_2$, 1 mM EDTA, 1 mM ThDP, and 20% ethylene glycol. Scans were recorded at 2.56 ms intervals. Traces 1−11 were acquired at 1.28, 14.1, 26.9, 39.7, 52.5, 78.1, 103.7, 229.1, 382.7, 561.9 and 2047 ms.

Rapid-Scan Stopped-Flow studies were carried out on an Applied Photophysics model SX.18MV stopped-flow spectrophotometer at 5.6 or 30 °C. Temperature was controlled with a Lauda MGW bath control. Diode-array spectral data were deconvoluted into separate intermediates using the Pro-Kineticist Software v. 1.03 from Applied Photophysics Ltd. Leatherhead, England. Data fitting was carried out with the SigmaPlot software from SPSS.

RESULTS AND DISCUSSION

Wild-Type BFD. It was first shown that NBFA is indeed a substrate for BFD. An experiment was carried out at 0.1 mM NBFA concentration with horse liver alcohol dehydrogenase and NADH confirming that NBFA was quantitatively converted to the *p*-nitrobenzaldehyde product in approximately 800 s at 25 °C. This provides an estimate of 0.004 s^{-1} for the first-order rate constant for substrate consumption (assuming 5 half-lives). The steady-state kinetic parameters were determined using a horse liver alcohol dehydrogenase/NADH-linked assay, providing a $K_m = 0.154$ mM and $k_{cat} < 0.04$ s^{-1} for NBFA (the value of k_{cat} being somewhat uncertain due to unavoidable spectral overlap of NADH and NBFA). These experiments clearly demonstrated that NBFA is a substrate for BFD.

The stopped-flow experiment involves mixing BFD in one syringe with the NBFA in the second syringe. To obtain good quality stopped-flow kinetic data the reaction was slowed by running the experiment at 5.6 °C. The typical concentration of BFD was 5.8 μM, and studies were initially carried out at pH 6.0 and 7.0. Ultimately, most data were collected at pH 7.0, since the extinction coefficient reporting on transient I_1 was considerably greater at the higher pH. A typical rapid-scan stopped-flow spectrum is shown in Figure 2. Deconvolution of the spectra into components is shown in Figure 3. There is evidence for the formation of two chromophoric transients (Figure 4) with λ_{max} 620 nm (I_1) and ~400 nm (I_2) and a chromophoric product with λ_{max} >730 nm (I_3) that is stable for the duration of the stopped-flow experiment.

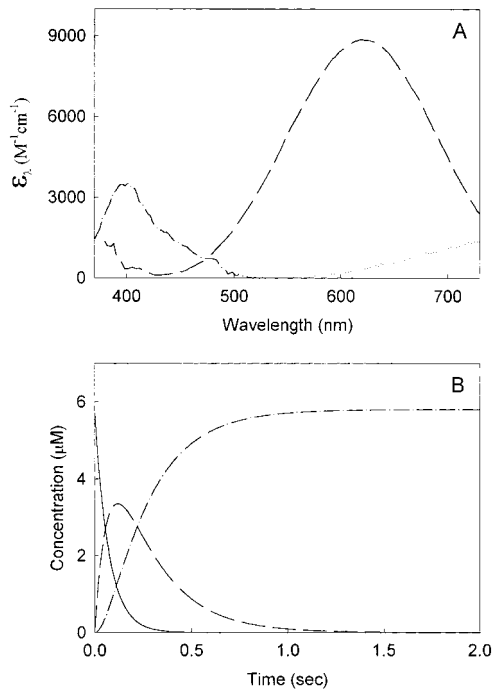

FIGURE 3: Deconvolution of transients in the rapid-scan spectra presented in Figure 2 according to a mechanism with two consecutive irreversible steps: E·NBFA $\rightarrow$ I_1 $\rightarrow$ I_2. Extinction coefficients (A) and concentration profiles (B) of the two intermediates I_1 (dashed line) and I_2 (dash−dotted line) represent best fit of the data in Figure 2 with the assumption that all enzyme is saturated with substrate in a Michaelis complex (solid line). Rate constants for the two irreversible reactions are equal to 13.23 ± 0.039 and 4.75 ± 0.010 s^{-1}. The spectrum of the product (dotted line) is shown for reference.

The first transient I_1 is formed and depleted in 1.0 s (see slice of A_{620} against time in Figure 4, panel B). We suggest that the absorbance reporting on I_1 represents a charge-transfer band for the following reasons. First, its wavelength maximum is certainly unexpected and very much higher than expected for any of the covalent intermediates envisioned, of which only the enamine is expected to be a good chromophore. The width and symmetrical appearance of the band are appropriate for a charge-transfer band. Second, its extinction coefficient is strongly pH-dependent, necessitating that data be collected at pH 7.0, for it is difficult to observe at pH 6.0. The same NBFA also gives rise to a band with λ_{max} near 550 nm when mixed with PDC, and the λ_{max} was shifted to longer wavelength by 40−50 nm upon addition of 10% (v/v) CH_3CN (*7*). Since the same intermediates should be formed on both enzymes, we assume that the local environment is perturbing the chromophore, and the dramatic perturbation on an absorption spectrum is most consistent with a charge-transfer band. We associate this charge-transfer band at 620 nm with NMThDP interacting with the enzyme. On account of the ϵ_{620} of ca. 9000, it is likely that it reflects intermolecular, rather than intramolecular electron transfer. This leaves the following possibilities (please note that neither the substrate nor the product possesses this band). (a) The C2-carbene/ylide (electron donor) of ThDP could interact with substrate (electron acceptor) in a Michaelis noncovalent complex. This is unlikely for at least two reasons: substrate-dependent formation of I_1 shows that substrate binding has already taken place prior to formation of I_1 (see kinetic analysis below), and the pH dependence of the amplitude of the effect, which suggests that some group undergoing change in ionization with a pK < 7 is interacting in its conjugate base form. This pK_a is more appropriate to a His than to the pK_a for thiamin. (b) The enamine (electron acceptor) itself with a His nearby (electron donor) gives rise to A_{620}, consistent with the pH dependence alluded to above. Since I_1 disappears with the same rate constant as the one characterizing the build-up of I_2 and since there are no conjugated intermediates past the enamine on the pathway, this scenario is unlikely. (c) Our choice is that NMThDP is the intermediate I_1 as the acceptor vis-à-vis H70 as donor (see section on the H70A variant below), with the resulting charge-transfer band at A_{620}. Also, the *m*-nitro derivative gave no spectrum under the same conditions on PDC (*7*). This assignment of the A_{620} is consistent with all of the of the observations so far. We wish to emphasize, however, that we use this charge-transfer band only as a reporter (a result of the *p*-nitro substituent on this alternate substrate) for the NMThDP intermediate, but certainly do not intend to imply that a charge-transfer complex is an obligatory intermediate in the mechanism.

Next, the concentration-dependence of the build-up and disappearance of I_1, the most prominent and best-defined chromophore, was examined. The NBFA concentration was in excess over BFD in all of these experiments, since the K_m is rather high for NBFA, as it is for benzoylformate (*9*−*12*). For fixed concentration of enzyme with variable concentration of NBFA, the first-order rate constants for the build-up and depletion exhibit saturation (Figure 5 and Table 1). For fixed concentration of NBFA (2 mM) and variable concentrations of BFD, the rate constants are the same (approximately 10 and 1.8 s^{-1}), while the maximum absorbance achieved at 620 nm varies in a linear fashion with BFD concentration up to 5 μM at pH 7.0 and 5.6 °C (data not shown). These experiments confirm that we are observing a BFD-bound species.

The second transient, I_2 at 5.6 °C appears to rise (Figure 4, panel C), then level off, while at 30 °C, it clearly shows slow depletion with time (not shown). The rate constant for build-up of this transient parallels, within experimental error, the rate constant for decrease of the I_1, strongly suggesting that the same event is monitored by the two relaxations. The λ_{max} for this transient is very near that expected for the enamine intermediate (*13*, *14*) with a *p*-nitro substituent.

The absorption corresponding to I_3 is built up at approximately the same rate as I_2, or slower; however, it persists at the same amplitude for the duration of the stopped-flow experiment (2 s). Given the unusual λ_{max} and very broad nature of the absorption band, it would be premature to speculate about its origins.

Next, relaxation kinetic theory (*15*) was used to interpret the transient kinetic observations. The reactions can be interpreted in terms of three relaxations: a fast one (non-saturable and too fast to measure with the stopped-flow instrument) involving binding of substrate, followed by $1/\tau_1$ forming NMThDP the first covalent complex between ThDP and NBFA, and finally $1/\tau_2$, corresponding to decarboxylation of NMThDP to the enamine. The data on I_1 allowed us to deduce rate constants from the $1/\tau_1$ and $1/\tau_2$ relaxations, as well as a dissociation constant for the Michaelis complex (see equations in the figure legends). Using the data between

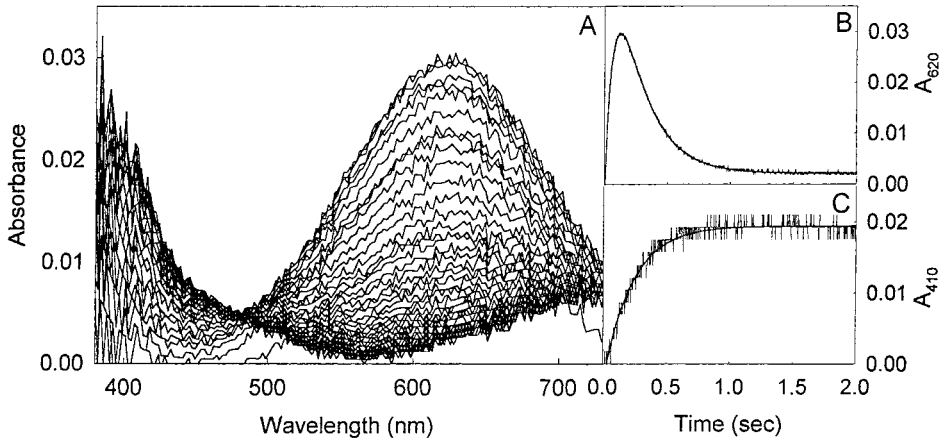

FIGURE 4: Difference spectra (A) and time course of the two intermediates I_1 (620 nm, panel B) and I_2 (410 nm, panel C). Conditions were the same as described in Figure 2. Calculated rate constants for the formation ($1/\tau_1$) and depletion ($1/\tau_2$) of I_1 are 13.83 ± 0.12 s^{-1} and 4.51 ± 0.028 s^{-1}, respectively. Rate constant for the formation of I_2 is 4.42 ± 0.060 s^{-1}.

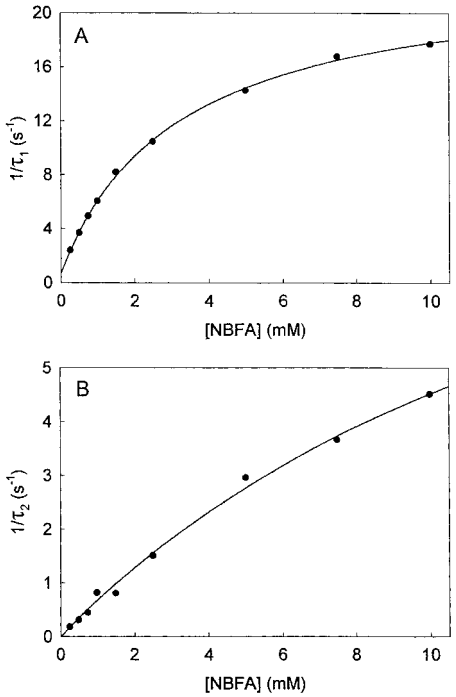

FIGURE 5: Dependence of the build-up (A) and depletion (B) of I_1 as a function of NBFA concentration. Conditions were the same as described in Figure 2. Solid lines represent the best fit of $1/\tau_1$ vs [NBFA] and $1/\tau_2$ vs [NBFA] according to the eqs $1/\tau_1 = k_2S/(K_{d1} + S) + k_{-2}$ and $1/\tau_2 = k_3S/(K_{d2} + S)$, respectively.

0.25 and 10 mM NBFA for 5.8 μM BFD, the parameters in Table 2 were deduced.

Similarly, the minimal mechanism to account for the observations invokes at least three steps. The dissociation constant K_{d1} for NBFA with wild-type BFD is 3.22 mM as compared to a K_m of 0.154 mM (see above and Polovnikova et al., manuscript in preparation).

As shown in Figure 5, the substrate concentration dependence of the $1/\tau_1$ relaxation indicates that the curve may have a nonzero *y*-intercept; hence the rate constant k_{-2} is most likely nonzero. At the same time, the magnitude of k_2 is not very sensitive to the assumption of zero or nonzero for k_{-2}. The rate constant k_2 is assigned to conversion of the BFD·ThDP·NBFA ternary (noncovalent) Michaelis complex to a covalent ThDP−substrate adduct, NMThDP, and the rate constant k_{-2} is assigned to its reversion to the Michaelis complex.

Table 1: Rate Constants for Build-up and Depletion of the Transient A_{620} on BFD When Reacted with *p*-Nitrobenzoylformic Acid at pH 7.0 and 5.6 °C

[NBFA] (mM)	$1/\tau_1$ (s^{-1})	$1/\tau_2$ (s^{-1})
0.25	2.39 ± 0.01	0.18 ± 0.003
0.50	3.69 ± 0.02	0.31 ± 0.005
0.75	4.95 ± 0.02	0.45 ± 0.004
1.0	6.05 ± 0.03	0.82 ± 0.01
1.5	8.19 ± 0.03	0.81 ± 0.01
2.5	10.47 ± 0.05	1.51 ± 0.01
5.0	14.27 ± 0.07	2.96 ± 0.01
7.5	16.79 ± 0.10	3.66 ± 0.01
10.0	17.72 ± 0.16	4.51 ± 0.03

The formation rate of I_2, attributed to the enamine, is identical to the rate of depletion of I_1 within the error of analysis. The most curious feature of the results is that the $1/\tau_2$ relaxation is also strongly substrate concentration-dependent. It is reasonable to assume, with no evidence to the contrary, that the rate constant k_{-3} is essentially zero, i.e., decarboxylation is irreversible. Hence, the only way to fit the totality of the findings is to assume that the decarboxylation step itself (k_3) is assisted by the substrate, in other words, the data were fit with a term $k_3[S]/(K_{d2} + [S])$. A plausible explanation of this finding is the notion reflected in Scheme 2, i.e., an "alternating sites" reaction pathway, according to which the site in a second subunit must be occupied by substrate before decarboxylation at the first site can be completed. According to this mechanism, the two ThDP sites must interchange their roles during the catalytic cycle. In a much slower reaction, the enzyme can also catalyze the decarboxylation with only a single site filled (k_3'). Enzymes such as BFD, which utilize ThDP, are subject to several regulatory mechanisms, such as hysteretic behavior vis-à-vis ThDP·Mg (II) (see ref 1) and, in several cases such as yeast PDC, very pronounced substrate activation. Therefore, it would not be totally unreasonable that BFD, a homotetrameric enzyme just as PDC, is also under regulatory control, albeit of a different origin. As shown below, the rate of formation of the transient attributed to the enamine is also concentration-dependent for the H70A variant, for which the transient I_1 cannot be observed, clearly supporting this apparent substrate-dependent behavior of k_3.

Table 2: Calculated Rate Constants for Scheme 2 for NBFA Reacting with BFD

	K_{d1} (mM)	k_2 (s^{-1})	k_{-2} (s^{-1})	K_{d2} (mM)	k_3 (s^{-1})	k'_3 (s^{-1})
wild type (5.6 °C)	3.22 ± 0.23	22.6 ± 0.37	0.73 ± 0.22[a]	17.1 ± 3.69	12.2 ± 1.86	<0.2
	2.68 ± 0.14	22.4 ± 0.46	0[b]			
H70A (30 °C)				10.5 ± 2.31	2.00 ± 0.23	0.073 ± 0.020

[a] Calculated assuming nonzero k_{-2}. [b] Calculated assuming zero k_{-2}.

Scheme 2: Decarboxylation of NBFA by BFD Requiring Two Active Sites

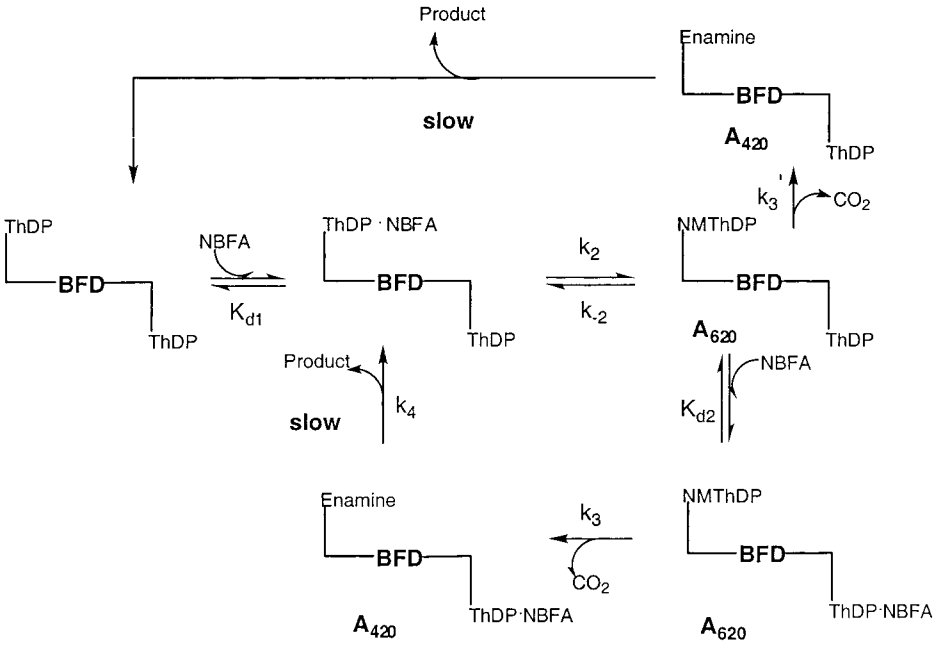

For the wild-type BFD, the first-order rate constant $k_3^{apparent}$ from the total analysis is ca. 4.5 s^{-1}. Under the same experimental conditions, $k_2^{apparent}$ is 13.8 s^{-1}, suggesting again that decarboxylation is slower than formation of the covalent NMThDP. On the other hand, the analysis also suggests that $k_3 > k_{-2}$, thereby indicating that primary carbon kinetic isotope effects for CO_2 release, measured under competitive (V/K) conditions, should give a number near unity. Indeed this is observed for benzoylformate decarboxylase (*12*) and, of course, the numbers unequivocally support the notion that product (benzaldehyde) release is rate-limiting overall.

The H70A BFD Variant. A rapid-scan stopped-flow spectrum resulting from the mixing of NBFA with this active center variant at 30 °C is shown in Figure 6. The experiments were run at a higher temperature, as this is a much-impaired variant [for benzoylformate, the specific activity and K_m are 260 U/mg and 0.37 mM for wild-type, and 1.1 U/ mg and 9.4 mM for the H70A variant, respectively (Polovnikova et al., manuscript in preparation)]. Most importantly, at the pH values used, for this variant, only I_2 and I_3 are observed, with no evidence of I_1. Again, the substrate dependence of I_2 buildup and breakdown was examined (Figure 7) and showed saturation with a nonzero *y*-intercept consistent with Scheme 2 (Table 3). The steady-state rate for conversion of I_2 to I_3 exhibits saturation with increasing NBFA concentration and provides a K_m of 2.91 ± 0.44 mM, the same value as obtained from steady-state kinetics with the natural substrate (Polovnikova et al., manuscript in preparation). This result strongly suggests that the *p*-nitro substitution on the NBFA affects transition state binding more than reactant binding.

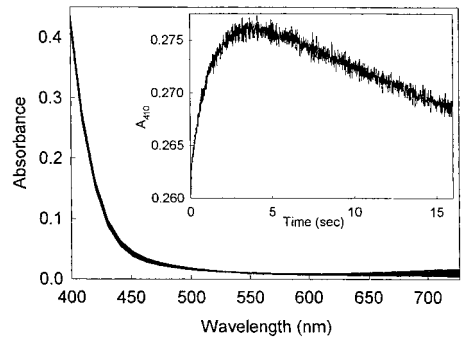

FIGURE 6: Rapid-scan stopped-flow trace of the H70A BFD variant reacting with *p*-nitrobenzoylformic acid at pH 7.0 and 30 °C. Concentration of the H70A BFD variant was 5.8 μM and that of NBFA was 5 mM. Reaction was carried out in the same buffer as used with wild-type BFD. Time-dependent change of absorbance at 410 nm is shown in the inset.

Perhaps the most remarkable finding is that this variant does not exhibit the charge-transfer band reporting on I_1 so prominent with the wild-type enzyme. The simplest explanation is that interaction of NBFA with His70 produces the charge-transfer band or, minimally, that His70 must be present and very likely in its neutral imidazole form for the charge-transfer band to exist. The latter deduction is because at pH 6.0 it was very difficult to observe I_1. As a bonus, the results suggest that there is a change in the fraction of H70 side chain ionization state giving rise to the charge-transfer band between pH 6 and 7. We also note that a superposition of active centers finds His70 near H115 of PDC (*9*), on which NBFA also produced such a charge-transfer band (*7*). Nevertheless, it is important to emphasize that the inability

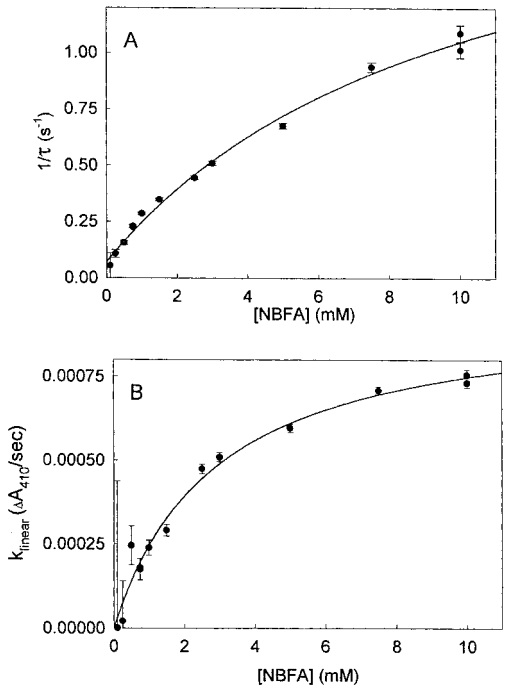

FIGURE 7: Dependence of the exponential build-up (A) and steady-state depletion (B) of I_2 as a function of NBFA concentration for the H70A BFD variant. Conditions were the same as in Figure 6. Fitting equation for $1/\tau$ vs [NBFA] is $1/\tau = k_3S/(K_{d2} + S) + k_3'$. The rate of steady-state depletion (k_{linear}) vs [NBFA] is fitted to the Michaelis−Menten equation.

Table 3: Rate Constants for Build-up and Depletion of the Transient I_2 on H70A BFD When Reacted with NBFA at pH 7.0 and 30 °C[a]

[NBFA] (mM)	$1/\tau$ (s^{-1})	k_{linear} (ΔA_{410}/sec)
0.1	0.053 ± 0.057	5.28e−7 ± 4.37e−4
0.25	0.107 ± 0.0184	2.07e−5 ± 1.19e−4
0.5	0.156 ± 0.0087	2.46e−4 ± 5.76e−5
0.75	0.229 ± 0.0075	1.75e−4 ± 3.21e−5
1.0	0.286 ± 0.0066	2.39e−4 ± 2.26e−5
1.5	0.348 ± 0.0064	2.91e−4 ± 1.74e−5
2.5	0.444 ± 0.0080	4.75e−4 ± 1.41e−5
3	0.509 ± 0.0101	5.09e−4 ± 1.39e−5
5	0.676 ± 0.0122	5.96e−4 ± 1.24e−5
7.5	0.937 ± 0.0220	7.09e−4 ± 1.17e−5
10	1.015 ± 0.0346	7.56e−4 ± 1.56e−5
10	1.089 ± 0.0361	7.32e−4 ± 1.47e−5

[a] Data analyzed according to the equation

$$A = A_1 e^{-t/\tau} + k_{lin} t + A_0$$

to observe the I_1 with A_{620} with the H70A variant in no way implies that the reaction pathway bypasses NMThDP.

A comparison of k_3 for wild-type (at 5.6 °C) and H70A variant BFD (at 30 °C) shows that the H70A substitution has a large effect on k_3 (for any reasonable activation energy used to estimate the rate constant for the wild-type enzyme at 30 °C), consistent with the finding of large effects on *V*/*K* with the natural substrate and rather little on the formation of I_3 and product release.

CONCLUSIONS

Several conclusions can be drawn from the results. First and foremost, the experiments confirm the existence and kinetic competence of the enamine as a highly conjugated species on the reaction pathway. The rate constants in Table 2, corrected to 30 °C and within experimental limits, would be consistent with the turnover number of the enzyme with the natural substrate. Second, the observations provide direct evidence for the nonconcerted nature of decarboxylation and product release, with product release being rate-limiting. Third, the rate constant for enamine formation is remarkably similar, again within a factor of 2, to that observed for the formation of the enamine from the conjugated substrates on PDC (*6*). Finally, the similarity of the rate constants on these two enzymes and of the turnover number for the related pyruvate oxidase (*19*) suggests that all of these ThDP enzymes share common features through decarboxylation. These include a large "solvent" effect, i.e., stabilization of the zwitterionic intermediates by the active center with a low apparent dielectric constant (*20*). We are led to this conclusion on the basis of observations that, on all ThDP enzyme structures determined so far, the coenzyme always assumes the same "V" conformation. Further, there are three highly conserved hydrogen bonds to the pyrimidine ring, prompting one of our groups to propose that the coenzyme carries out the bulk of the work through decarboxylation (*21*). In fact, other than the conserved "V" conformation and the three conserved hydrogen bonds, the active centers appear to be significantly different in PDC and BFD (*9*), notwithstanding very similar functions through decarboxylation. One may reasonably speculate that the conserved structural features provide the bulk of the enzymatic rate acceleration. Indeed, substitution of other groups at the active center (*1*, *22*, *23*) accounts for only 10^2-10^4-fold rate accelerations on either enzyme. The fast spectroscopic detection of the fate of key enzymatic intermediates offers a method for comparison of catalysis on this enzyme with different amino acid substitutions.

ACKNOWLEDGMENT

E.S. and F.J. gratefully acknowledge helpful discussions regarding charge-transfer spectroscopy with Piotr Piotrowiak.

REFERENCES

1. Jordan, F., Nemeria, N., Guo, F., Baburina, I., Gao, Y., Kahyaoglu, A., Li, H., Wang, J., Yi, J., Guest, J. R., and Furey, W. (1998) *Biochim. Biophys. Acta 1385*, 287−306.
2. Dyda, F., Furey, W., Swaminathan, S., Sax, M., Farrenkopf, B., and Jordan, F. (1993) *Biochemistry 32*, 6165−6170.
3. Arjunan, P., Umland, T., Dyda, F., Swaminathan, S., Furey, W., Sax, M., Farrenkopf, B., Gao, Y., Zhang, D., and Jordan, F. (1996) *J. Mol. Biol. 256*, 590−600.
4. Kuo, D. J., and Jordan, F. (1983) *J. Biol. Chem. 258*, 134l5−13417.
5. Zeng, X., Chung, A., Haran, M., and Jordan, F. (1991) *J. Am. Chem. Soc. 113*, 5842−5849.
6. Menon-Rudolph, S., Nishikawa, S., Zeng, X., and Jordan, F. (1992) *J. Am. Chem. Soc. 114*, 10110−10112.
7. Zeng, Xiaoping, (1992) Ph.D. Dissertation, Rutgers University Graduate Faculty at Newark.
8. Jordan, F., Kudzin, Z. H., Rios, C. B. (1987) *J. Am. Chem. Soc. 109*, 4415−4416.
9. Hasson, M. S., Muscate, A., McLeish, M. J., Polovnikova, L. S., Gerlt, J. A., Kenyon G. L., Petsko, G. A., and Ringe, D. (1998) *Biochemistry 37*, 9918−9930.
10. Hegeman, G. D. (1970) *Methods Enzymol. 17A*, 674−678.
11. Reynolds, L. J., Garcia, G. A., Kozarich, J. W., and Kenyon, G. L. (1988) *Biochemistry 27*, 5530−5538.
12. Weiss, P. M., Garcia, G. A., Kenyon, G. L., Cleland, W. W., and Cook, P. F. (1988) *Biochemistry 27*, 2197−2205.

13. Barletta, G. L., Huskey, W. P., and Jordan, F. (1992) *J. Am. Chem. Soc. 114*, 7607−7608.
14. Barletta, G. L., Huskey, W. P., and Jordan, F. (1997) *J. Am. Chem. Soc. 119*, 2356−2362.
15. Bernasconi, C. F. (1976) *Relaxation Kinetics*, pp 20−75, Academic Press, New York.
16. Bradford, M. M. (1976) *Anal. Biochem. 86*, 142−146.
17. Hasson, M. S., Muscate, A., Henehan, G. T. M., Guidinger, P. F., Petsko, G. A., Ringe, D., and Kenyon, G. L. (1995) *Protein Sci. 4*, 955−959.
18. Tsou, A. Y., Ransom, S. C., Gerlt, J. A., Buechter, D. D., Babbit, P. C., and Kenyon, G. L. (1990) *Biochemistry 29*, 9856−9862.
19. Bertagnolli, B., and Hager, L. P. (1991) *J. Biol. Chem. 266*, 10168−10173.
20. Jordan, F., Li, H., and Brown, A. (1999) *Biochemistry 38*, 6369−6373.
21. Guo, F., Zhang, D., Kahyaoglou, A., Farid, R. S., and Jordan, F. (1998) *Biochemistry 37*, 13379−13391.
22. Liu, M. et al., manuscript in preparation on pyruvate decarboxylase.
23. Polovnikova, E. et al., manuscript in preparation on benzoylformate decarboxylase.

BI001214W